A neural circuit for spatial orientation derived from brain lesions

Moshe Roseman, MD,[1,†] Uri Elias, BS,[1,†] Isaiah Kletenik, MD,[2,3,4] Michael A. Ferguson, PhD,[2,3] Michael D. Fox, MD, PhD,[2,3] Zalman Horowitz, MD,[1] Gad A. Marshall, MD,[3,4,5,6] Hugo J. Spiers, PhD[7] and Shahar Arzy, MD, PhD[1,8,9]

† **These authors contributed equally to this work.**

Author affiliations:

1 Neuropsychiatry Lab, Department of Medical Neurosciences, Faculty of Medicine, Hadassah Ein Kerem Campus, Hebrew University of Jerusalem, Jerusalem 9112001, Israel

2 Center for Brain Circuit Therapeutics, Departments of Neurology, Psychiatry, and Radiology, Brigham & Women's Hospital, Boston, Massachusetts 02115, USA

3 Harvard Medical School, Boston, Massachusetts 02115, USA

4 Division of Cognitive and Behavioral Neurology, Department of Neurology, Brigham and Women's Hospital, Boston, Massachusetts 02115, USA

5 Center for Alzheimer Research and Treatment, Department of Neurology, Brigham and Women's Hospital, Boston, Massachusetts 02115, USA

6 Department of Neurology, Massachusetts General Hospital, Boston, Massachusetts 02114, USA

7 Institute of Behavioural Neuroscience, Department of Experimental Psychology, University College London, London WC1H 0AP, UK

8 Department of Neurology, Hadassah Hebrew University Medical School, Jerusalem 9112001, Israel

9 Department of Brain and Cognitive Sciences, Hebrew University of Jerusalem 9190501, Israel

Abstract

There is disagreement regarding the major components of the brain network supporting spatial cognition. To address this issue, we applied a lesion mapping approach to the clinical phenomenon of topographical disorientation. Topographical disorientation is the inability to maintain accurate knowledge about the physical environment and use it for navigation. A review of published topographical disorientation cases identified 65 different lesion sites. Our lesion mapping analysis yielded a topographical disorientation brain map encompassing the classic regions of the navigation network: medial parietal, medial temporal and temporo-parietal cortices. We also identified a ventromedial region of the prefrontal cortex, which has been absent from prior descriptions of this network. Moreover, we revealed that the regions mapped are correlated with the Default Mode Network sub-network C. Taken together, this study provides causal evidence for the distribution of the spatial cognitive system, demarking the major components and identifying novel regions.

Running title: Lesion-based spatial orientation network

Keywords: navigation; disorientation; network; connectivity; space

Introduction

Neural processing of spatial cognition and navigation has garnered much interest in recent decades (Burgess et al. 2002; Buzsáki and Moser 2013; Epstein et al. 2017). The seemingly simple task of moving in space towards a remembered location requires representations of both the environment (including its size, structure, borders and embedded landmarks) and oneself, as well as a mechanism for continuously updating self-location (Tolman 1948; O'Keefe and Nadel 1978; Burgess et al. 2002; Vogeley and Fink 2003; Doeller et al. 2010; Buzsáki and Moser 2013; Epstein et al. 2017; Bicanski and Burgess 2018). One major cognitive mechanism that supports these representations is cognitive maps. Cognitive maps are defined as "schematic-like mental representation of the relationships between entities in the world" (Arzy and Schacter 2019). These maps code for different aspects of spatial navigation, as based on an ensemble of specific cells, located mainly in the hippocampus and nearby medial temporal regions. These include cells aiming to identify a specific location (place cell), angle (head direction cells), distance (vector cells), velocity (speed cells) or border of the environment (border cells), as well as cells creating a grid pattern across the environment (grid cells) (for review see Behrens *et al.* (Behrens et al. 2018)).

For one to utilize a cognitive map to guide navigation, the map's coordinates must be anchored to stable real-world landmarks (Epstein et al. 2017). These landmarks act as environmental cues that are critical for calibrating the orientation and displacement of the cognitive map. It has been shown that the parahippocampal place area (PPA) and occipital place area (OPA) are key regions for the perception and visual recognition of landmarks (Epstein and Kanwisher 1998; Dilks et al. 2013). Additionally, the retrosplenial cortex (RSC) has been associated with using landmarks to anchor the cognitive map (Vann et al. 2009; Marchette et al. 2015). This has a special importance for path integration, a body-centered egocentric strategy of combining

direction and velocity into an aggregate of routes that in turn give rise to the cognitive-map representation. It is the RSC which predominantly mediates the online transition between "egocentric" and "allocentric" reference frames, thereby enabling one to stay oriented during navigation (Lambrey et al. 2012; Marchette et al. 2015). Finally, another important region that may be involved in the context of the navigating self is the medial prefrontal cortex (mPFC) (Arzy and Schacter 2019; Patai and Spiers 2021), yet its involvement is only rarely mentioned in studies of spatial cognition, usually with respect to planning or imagining potential goals (Balaguer et al. 2016; Javadi et al. 2019). Very few studies have mentioned the mPFC in the context of situating the self with respect to the environment (Wolbers et al. 2007; Kumaran et al. 2016), suggesting a central role for this brain region in navigation.

To account for the different processes involved in spatial cognition and navigation, we have adopted a clinical approach, based on the clinical phenomenon of topographical disorientation (TD) and lesion network analysis. TD is defined as "a loss of the ability to find one's way within large-scale, locomotor environments" (Habib and Sirigu 1987; Aguirre and D'Esposito 1999). In a comprehensive review, Aguirre and D'Esposito suggested TD to include deficits in spatial processing of visual information (landmark agnosia) (Takahashi and Kawamura 2002; van der Ham et al. 2017), mentally representing locations with respect to the self (egocentric disorientation) (Stark et al. 1996), estimating distances and directions (heading disorientation) (Hashimoto et al. 2010) and acquiring new environmental information (anterograde disorientation) (Habib and Sirigu 1987). As Aguirre and D'Esposito noticed, these diverse clinical presentations of TD may be the results of brain lesions in multiple different brain regions that contribute to spatial cognition. Hence, attempts to define the cortical contributors to spatial cognition by simply overlapping brain lesions are likely to fail. The recently developed lesion network mapping technique (Fox 2018) builds on the assumption that lesions in various brain regions, which are connected to a common brain network, may result in a

similar clinical symptom (Boes et al. 2015; Fox 2018; Darby et al. 2019; Kletenik et al. 2022; Siddiqi et al. 2022; Kletenik, Cohen, et al. 2023). In this vein, we hypothesized that the connectivity profile of brain lesions underlying TD will map to a comprehensive brain network; that this network will be specific to TD versus other lesion induced symptoms; and that this network will align with imaging correlates of spatial cognition and navigation.

Materials and Methods

Lesion identification

To find case reports of patients who experienced spatial disorientation, a search was performed on January 16, 2020 using the PubMed database. The query required a combination of a disorientation search term ("spatial disorientation" or "disorientation for place" or "disorientation for space" or "topographical disorientation" or "heading disorientation") and a term indicating a brain lesion ("lesion" or "stroke" or "infarct" or "ischemia" or "hemorrhage" or "tumor"). This query returned 544 results, of which 413 were available and in English. These abstracts were reviewed, and the following inclusion criteria were applied: 1. at least one of the “disorientation” terms from the search query is mentioned as a symptom; 2. the symptoms are attributed to a brain lesion; and 3. a clear image of the lesion is included in the paper. Exclusion criteria were: 1. abnormal brain anatomy due to either a chronic condition or an acute lesion; 2. the provided image does not correspond to the axial, sagittal or coronal plane of the MNI152 template; and 3. the patient is under 16 years of age. Fifty-four articles fulfilled these criteria. In those articles, 65 unique spatial disorientation cases were identified (mean age 62.05 ± 12.6 years, range 31-83, 81.8% male), most of them (56) being the result of an ischemic or

hemorrhagic stroke. In 23 of these cases, TD was the only symptom; in two cases it was accompanied by temporal disorientation; and 40 cases presented with additional symptoms, including visual, executive and mnemonic deficiencies (Table S1).

Lesion Tracing

Brain lesions were mapped by hand onto a standardized template brain (MNI152 T1 1mm brain, http://fsl.fmrib.ox.ac.uk/fsldownloads/), using FSLeyes (https://zenodo.org/record/5576035) consistent with prior lesion network mapping studies (Boes et al. 2015; Ferguson et al. 2019; Kletenik et al. 2022; Kletenik, Gaudet, et al. 2023). Lesions were traced in two dimensions according to the plane of the published brain image, using neuroanatomical landmarks to accurately transfer the lesion location onto the template brain (Fig. 2A). Mapping was performed by M.R. and reviewed for accuracy by board-certified neurologist S.A.. All images used are publicly available.

Lesion network mapping

Following the method developed by Fox *et al.* (Fox 2018), a brain network was identified for each lesion according to its resting-state functional connectivity (RSFC). The estimation of the RSFC maps was based on resting-state fMRI scans of healthy young adults collected by the FCon1000 project (http://fcon_1000.projects.nitrc.org/fcpClassic/FcpTable.html). As previously shown, this choice is equivalent to using older, age-matched individuals (Fox et al. 2014; Boes et al. 2015). Scans from various sites, scanners and protocols were randomly chosen and downloaded from the project until results were stable (adding the last 100 scans resulted in negligible changes to the results); 419 resting-state scans were eventually used (39% males, ages 18–44 years). The resting-state fMRI scans, together with their respective T1 images, were preprocessed using SPM12 and DPARSFA (Yan and Zang 2010), with slice time and motion

correction, linear normalization, scrubbing, regression with white-matter and CSF signals, as well as motion and motion derivatives, time domain filtration to 0.01-0.1Hz band and 4 mm Gaussian spatial filtering.

Each of the 65 lesions was used as a seed for the preprocessed resting-state fMRI scans, which were then averaged to create 65 BOLD signals. The BOLD signals were then correlated to each grey matter voxel in each resting-state fMRI scan, to yield 65x419 cortical maps of Pearson correlation coefficients. The correlation maps of each lesion were *Z*-scaled, averaged and thresholded using a data-driven threshold (see below) set at *Z*-score = ±0.27 to generate 65 lesion connectivity maps (Fig. 2B). In cases of several spatially disconnected lesions, to account for the different connectivity patterns, this procedure was repeated for each lesion separately, and the maximal value was chosen for each voxel of the connectivity map ("maximal component connectivity"). Next, the connectivity maps were binarized and summed to obtain a single map of shared lesion connectivity. Repeating the analysis using only the 23 cases with pure TD symptoms produced an equivalent map.

To choose a data-driven connectivity threshold, we used a connectional homogeneity measure (Gordon et al. 2016). We applied the measure on two parcellations of the cortical surface, one into seven and one into seventeen networks (Yeo et al. 2011). We used the threshold we obtained for the seventeen networks, which was *Z*-score = ±0.27, more stringent than that of the seven networks parcellation which was *Z*-score = 0.21. Similar results were obtained when applying more stringent or relaxed thresholds.

Sensitivity and specificity testing

The lesion connectivity overlap map was thresholded to identify voxels connected to most of the TD-causing lesions. To assess the specificity of our results, we compared network maps from lesions causing TD to network maps similarly derived from 2-dimensional lesions

identified in the literature but which caused neurological syndromes other than TD (n = 507), including akinetic mutism, alien limb, aphasia, asterixis, cervical dystonia, criminality, freezing of gait, hemichorea, post-stroke pain, parkinsonism, prosopagnosia, depression, Holmes tremor, mania, peduncular hallucinosis, auditory, visual and mixed hallucinations (Boes et al. 2015; Laganiere et al. 2016; Fasano et al. 2017; Darby, Horn, et al. 2018; Darby, Joutsa, et al. 2018; Joutsa et al. 2018; Cohen et al. 2019; Corp et al. 2019; Joutsa et al. 2019; Padmanabhan et al. 2019; Cotovio et al. 2020). We did not include amnesia-related lesions due to the close similarity between spatial and temporal cognition, as well as co-occurrence of these two in the patients' group (Hartley et al. 2014; Peer et al. 2015; Peters-Founshtein et al. 2018; Dafni-Merom et al. 2019). FSL PALM (https://fsl.fmrib.ox.ac.uk/fsl/fslwiki/PALM) was used to perform a voxel-wise permutation-based two sample two-tailed *t*-test, using a threshold of false discovery rate (FDR)-corrected $p < 0.01$.

To identify a network that is both sensitive and specific to TD, a conjunction between the seed from the sensitivity map (voxels connected to >63% of TD-causing lesions) and the specificity map was computed as the overlap between the two (Fig. 2C). The resulting seed was used to define a network which encompasses lesion locations causing TD while avoiding control lesion locations. Functional connectivity with the seed was computed using the same methods as described for the lesions earlier. This method to derive a network from the functional connectivity of a peak seed has been applied in lesion network mapping analyses of other diverse syndromes including memory (Ferguson et al. 2019), depression (Padmanabhan et al. 2019) and religiosity (Ferguson et al. 2021). The resultant 419 correlation maps were further *Z*-scaled, averaged, and thresholded using the same connectivity threshold to receive the TD connectivity map (Fig. 2D). Clusters of local maxima and minima in the TD-map were identified using FSL's *cluster* tool.

Comparison to previous maps of spatial cognition and to cortical networks

Next, we compared our results to three brain maps of spatial cognition: (1) results of a meta-analysis performed via the Neurosynth database (http://neurosynth.org/), using the term 'Navigation' (Dafni-Merom and Arzy 2020); (2) regions that are associated with spatial orientation, as identified by a group analysis of 16 participants who made judgements regarding their distance from places vs. a lexical control task (Peer et al. 2015); (3) scene-selective brain regions that represent group activation clusters from 30 participants who watched images of scenes vs. images of objects (Julian et al. 2012) (http://web.mit.edu/bcs/nklab/GSS.shtml). After computing the voxelwise overlap percentage, volumes were mapped onto a group-averaged structural surface based on 1,200 healthy participants provided by the Human Connectome Project (HCP) using trilinear volume interpolation, and displayed using Connectome Workbench 1.5.0 (Marcus et al. 2011). The overlap between the TD-map and each of these maps was calculated using intersection over union (Jaccard index). To assess the statistical significance of the overlap, we used 7,000 task-related activations stored in the Neurosynth database. Since the database stores only the cluster coordinates of each contrast, we reconstructed each contrast using superposition and smoothing, repeating this process with multiple filters (FWHM = 8, 16, 24 mm) and thresholds with similar results. The Jaccard index was calculated for each of these contrasts to assess their overlap with the spatial cognition brain map, and this value was compared to that of the TD-map to obtain a *p*-value.

Finally, we compared our results to a parcellation of 17 cortical networks (Yeo et al. 2011), and for each network calculated the mean functional connectivity between the thresholded TD-map and the average resting-state fMRI BOLD signal masked by the cortical network. To control for mask size (and since connectivity, though thresholded, is not binary), we fitted the

threshold separately for each cortical network to maximize the Jaccard index, while keeping it above the minimal threshold of *Z*-score = 0.27. Statistical significance was assessed by permutation tests that randomized the location of the seed over the cortex and calculated the respective connectivity map and the connectivity to each of the cortical networks. One thousand random seeds were generated. Since the connectivities to the networks is not uncorrelated, we corrected for multiple comparisons by taking the highest connectivity as a reference to all networks. Cortical networks were visualized alongside our results as before.

Data availability

The TD-map, as well as the orientation map and the meta-analysis-based map, are available for download at https://github.com/CompuNeuroPsychiatryLabEinKerem, as well as our code for lesion network mapping analysis in a Jupyter Notebook. Scene-selective regions can be found at http://web.mit.edu/bcs/nklab/GSS.shtml

Results

Identifying brain lesions underlying topographical disorientation

We identified 65 cases of clinical topographical disorientation in the literature (Fig. 1. See Table S1 for lesion, etiology and patient details). Lesion locations were distributed across multiple brain regions, including the hippocampal-entorhinal system (31 lesions), the RSC (35 lesions) and the PPA (22 lesions). Less frequently involved regions include the lingual gyrus (six lesions), the posterior cingulate cortex (PCC, four lesions), the precuneus (four lesions),

the OPA (three lesions) and the parieto-occipital sulcus (two lesions). No lesions were found in the frontal cortex.

Mapping the brain network underlying topographical disorientation

Next, using functional connectivity analysis, we extracted the network of brain regions functionally connected to each lesion location (Fig. 2A-B). Despite the heterogeneity of lesion locations, 41 of the 65 functional connectivity networks (63%) overlapped in a common seed at the right parieto-occipital sulcus (Fig. 2C).

To ensure the specificity of this seed we performed a voxelwise two-sample t-test comparing the network maps of the TD lesions to network maps of controls. As controls we employed lesions from 507 patients similarly derived from lesions identified in the literature but which caused neurological syndromes other than TD (n = 507) (Boes et al. 2015; Laganiere et al. 2016; Fasano et al. 2017; Darby, Horn, et al. 2018; Darby, Joutsa, et al. 2018; Joutsa et al. 2018; Cohen et al. 2019; Corp et al. 2019; Joutsa et al. 2019; Padmanabhan et al. 2019; Cotovio et al. 2020). The same region surrounding the parieto-occipital sulcus was implicated in the TD network maps significantly more than in the other syndromes ($p < 0.001$, FDR-corrected), indicating the specificity of this location to TD (Fig. S1, Table S2). Whole-brain functional connectivity with this seed was used to define a brain network that is both sensitive and specific to spatial navigation (TD-map, Fig. 1D) as this network will intersect lesion locations causing TD while avoiding lesions not causing TD. In addition to the right parieto-occipital sulcus, this network includes mainly the precuneus, PCC, RSC, parahippocampal gyrus (PHG), hippocampus, angular gyrus and mPFC bilaterally (for full list see Table 1).

Table 1 Clusters of significant functional connectivity with the topographical disorientation seed

Cluster location	Volume (number of 1 mm^3 voxels)	x	y	z	z-score
Positive functional connectivity					
Bilateral medial parietotemporal cortex, R hippocampus*	1693	0	-54	15	1.46
Bilateral ventromedial prefrontal cortex	286	0	48	-9	0.48
L temporoparietal junction	178	-39	-75	33	0.432
R temporoparietal junction	165	45	-66	33	0.418
R superior frontal sulcus	36	24	30	42	0.327
L hippocampus	18	-21	-18	-18	0.351
L superior frontal sulcus	18	-21	27	42	0.318
R superior temporal sulcus	11	60	0	-18	0.312
Negative functional connectivity					
R anterior insula	40	54	18	0	-0.333
R temporoparietal junction	39	60	-39	42	-0.302
L temporoparietal junction	3	-60	-42	36	-0.278

Coordinates specify center of gravity (MNI space).

*The first cluster encompasses several brain regions, including medial parietal (parieto-occipital sulcus, retrosplenial cortex, precuneus, posterior cingulate cortex) and medial temporal (parahippocampal gyrus) components, as well as the right hippocampus, giving rise to a larger cluster with a less informative peak-value, unlike the rest of the clusters that contain a single brain region.

Relation of the TD-map to spatial cognition networks

To test whether our network derived from lesions aligns with imaging correlates of spatial cognition, we compared the TD-map to previously published spatial cognition-related brain maps, namely (1) a meta-analysis of task-based fMRI studies of spatial cognition and navigation, and available brain maps from previous studies of (2) spatial orientation and (3) scene-perception. First, we compared the TD-map to a meta-analysis of 77 navigation-related research articles performed via the Neurosynth database (https://neurosynth.org/ (Dafni-Merom and Arzy 2020); see also Epstein *et al.* (Epstein et al. 2017)) (Fig. 3A). Notably, though most of the brain regions included in the TD-map were also implicated in the meta-analysis, two brain regions were identified only by the current analyses: the PCC and the mPFC (Jaccard Index (JI) = 0.12, p = 0.06). Conversely, some regions were identified by the meta-analysis and did not appear in the current network lesion map, namely the dorsal precuneus, the collateral sulcus, the entorhinal cortex, a part of the lateral occipital cortex and several parts of the cerebellum.

We also compared the TD-map to brain activity during a spatial orientation task, obtained via high resolution (7T) fMRI (Peer et al. 2015). This analysis showed the TD-map to contain most of the spatial orientation map (JI = 0.26, p = 0.002, Fig. 3B). Finally, we compared our results to a map created from three masks of scene-selective brain regions: RSC, PPA and OPA, as identified by participants' responses to a places > objects contrast. (Julian et al. 2012) This analysis showed significant overlap for RSC and PPA (JI = 0.27, p = 0.007, Fig. 3C). However, a third scene-selective region, the OPA, had less overlap with the TD-map.

Relation of the TD-map to the default mode network

The ensemble of mPFC, medial parietal (mP) cortex, medial temporal lobe (MTL), and the temporoparietal junction (TPJ) gives rise to the default mode network (DMN), a prominent brain network related to self-reference and internal-mentation (Buckner et al. 2008), which is not usually related to spatial cognition, with the exception of a few proposals (Buckner and Carroll 2007; Spreng et al. 2009). To investigate the role of the DMN in spatial cognition, we compared the TD-map to a parcellation of the brain into 17 cortical resting-state fMRI networks, as identified in data from 1,000 participants (Yeo et al. 2011). The 17 networks parcellation includes a subdivision of the DMN to three specialized subnetworks. A subdivision of the DMN, Default C, showed significant functional connectivity with the TD-map (Fig. 4). This functional connectivity survived correction for multiple comparisons taking the highest connectivity as reference (see Methods), implying that the TD-map contains the core of the Default C signal. Other networks did not show significant connectivity with the TD-map.

Finally, three clusters exhibited significant negative connectivity with the TD seed. These were located in anterior parts of the TPJ bilaterally, and in the right anterior insula (Table 1). These regions are part of the 'Salience' or 'Ventral attention' network, one of several that commonly show negative correlation with the DMN (Yeo et al. 2011; Margulies et al. 2016).

Discussion

Building on the clinical phenomenon of TD, we identified 65 cases from the literature and employed the novel method of lesion network mapping to map a spatial orientation brain system ("TD-map"). On the clinical/phenomenological level, TD comprises a variety of spatial cognition disorders such as egocentric, heading, and anterograde disorientation, and landmark agnosia. On the neuroanatomical level, the TD-map includes brain activations in the medial

posterior parietal cortex (mPPC), mPFC, MTL and the TPJ. Notably, the mPFC and the precuneus part of the mPPC identified in our study were not shown in previous studies. Finally, a comparison of the TD-map to subnetworks of the DMN showed overlap mostly with Default C and Default A with no involvement of Default B. The DMN has been extensively implicated in Alzheimer's disease (AD) and its pathology (Greicius et al. 2004; Buckner et al. 2005; Buckner et al. 2009), and deficits in spatial cognition and navigation have similarly been demonstrated in early stages of AD (Kunz et al. 2015; Coughlan et al. 2018; Peters-Founshtein et al. 2018). Therefore, our findings may serve as a clinically meaningful cognitive and neuroanatomical signature for early-stage AD.

Several attempts have been made to pin down the brain system that underlies the multifaceted human spatial cognition and navigation. The most extensive system was borne out by two meta-analyses of human neuroimaging studies included in the Neurosynth database (Epstein et al. 2017; Dafni-Merom and Arzy 2020), comprising brain regions at the MTL, RSC, mPPC, lateral parietal and occipital lobe. Two other studies provided masks labelled as “spatial orientation” at the parieto-occipital sulcus, RSC and TPJ (Peer et al. 2015) and “scene perception” at the RSC, PPA and OPA (Julian et al. 2012). Of these four prior studies, only one meta-analysis showed involvement of the mPFC, though to a minimal extent (Dafni-Merom and Arzy 2020). This is notable since neuroimaging evidence has implicated the mPFC in several aspects of spatial cognition, including route planning (Spiers and Maguire 2006; Sherrill et al. 2013; Balaguer et al. 2016; Kaplan et al. 2017; Javadi et al. 2019) and path integration (Wolbers et al. 2007; Chrastil et al. 2017). Grid-like activity has also been found in the mPFC during virtual navigation in humans, further implicating a role for this region in spatial cognition (Doeller et al. 2010; Horner et al. 2016). In addition, a case study of a patient with ventromedial PFC damage was found to have difficulty navigating to familiar locations (Ciaramelli 2008) and it has been suggested this region may be important for spatial schemas to aid navigation in

familiar environments (Farzanfar et al. 2022). Our method and results thus provide further distinct evidence for the involvement of the ventral mPFC in the spatial cognitive system.

Another difference between the TD-map and the other spatial-cognition maps regards the mPPC. All maps showed involvement of the RSC; however, only the TD-map involved the ventral precuneus region as well. The precuneus has been shown to relate to mental navigation (Ghaem et al. 1997; Spiers and Maguire 2006; Spreng et al. 2009; Chadwick et al. 2015), spatial memory (Frings et al. 2006; Epstein et al. 2007), and distance coding (Patai et al. 2019). Moreover, a recent study focused on the anatomical distribution of the processing of different spatial scales found a cortical gradient of activity in the mPPC, in which the immediate environment activated posterior regions and larger spatial scales activated anterior regions, including the precuneus (Peer et al. 2019). It was suggested that this anterior part of the gradient, while originally not at the core of the spatial cognitive system, may be recruited for more extensive spatial computations. Accordingly, providing a more comprehensive picture of spatial cognition, the TD-map includes this part of the system as well.

Also implicated in the TD-map are components of the MTL and the TPJ. The MTL is consistently activated during tasks that involve an allocentric representation of space (Burgess et al. 2002; Ranganath and Ritchey 2012). Additionally, the TPJ is essential for egocentric perspective taking (Aguirre and D'Esposito 1999; Ruby and Decety 2001; Vogeley and Fink 2003), which has led several models of human spatial cognition to focus on the flow of information between these regions (Byrne et al. 2007; Bicanski and Burgess 2018; Arzy and Schacter 2019). In the current study, we have demonstrated that the TD-map contains both the MTL and the TPJ and hence reinforces these previous models. Notably, the parts of the MTL that are implicated in the TD-map are the hippocampus and the PHG, while more anterior components such as the perirhinal cortex are not implicated. The distinction between these posterior and anterior regions is the basis of a prominent theory that defines two cortical

systems for memory (Ranganath and Ritchey 2012). One system contains the PHG as well as posteromedial (PM) components, and is involved in processing contextual information for episodic memory, supplying the spatial, temporal and other underpinnings for stored events and referencing it to the perspective of one's self; the other system contains the perirhinal cortex and other anterior temporal (AT) components, and is involved in locating different entities in these multidimensional spaces and encoding the salience and values of these entities. This model suggests a central role for the PM system in spatial navigation, integrating one's perspective with the global spatial context into a first-person spatial representation. Our results highlight components of the PM system but not the AT system, which lends support to the anatomical and functional separation attributed to the two proposed systems.

When compared to a parcellation of cortical networks, the TD-map was found to have the largest overlap and strongest connectivity with subnetworks of the DMN. This is not surprising; previous findings have consistently implicated the DMN regions in spatial functions such as navigation (Maguire 2001; Burgess et al. 2002; Spreng et al. 2009; Dafni-Merom and Arzy 2020) spatial orientation (Peer et al. 2015; Peer et al. 2019), and scene construction (Hassabis and Maguire 2007). Though the functional difference between the DMN subnetworks is not fully understood, Default A is associated with social functions such as theory of mind while Default C is associated with episodic memory and spatiotemporal functions (Andrews-Hanna et al. 2014; Peer et al. 2015). Due to the close overlap between spatial and temporal cognition, and the fact that symptoms in these two faculties co-occurred in some of the patients, we did not include amnesia-related lesions in the control group of the specificity analysis. The separation between Default A and C is also consistently reflected in parcellation of the DMN into two subnetworks in the single subject level, yielding one network that is implicated in social cognition and another that is implicated in episodic memory (Braga et al. 2019; DiNicola et al. 2020). We therefore hypothesized that the TD-map would overlap Default C. While this

is indeed what we found, we also found connectivity (albeit not statistically significant) with Default A. This result may reflect the close interrelations between the spatial and social domains, that have been recently suggested to rely on similar cognitive mechanisms that work in tandem to assist both functions (Tavares et al. 2015; Park et al. 2020; Son et al. 2021; Arzy and Kaplan 2022). Further research is needed to explore the interrelations in between spatial and social orientation and the functional role of this conjunction.

Since its first introduction, the lesion network mapping technique has yielded brain circuits for episodic memory, depression, criminal behavior among other cognitive and mental domains (Darby, Horn, et al. 2018; Ferguson et al. 2019; Padmanabhan et al. 2019). The ability to derive information from a large body of individual patients was shown to be a rich source of knowledge for cognitive science (Fox 2018). This effort therefore extends the neurological tradition of meaningful deduction from single case studies to a newer, comprehensive level. Building on brain lesions that brought about clinical disorders enables inferring a causal link between the implicated brain regions and the impaired cognitive mechanisms. In addition, comparison of these lesion to incidental lesions that caused other disorders may determine the anatomical specificity of this causal link. As a result, this type of study ranks high on the causality continuum, outshined only by studies that involve targeted manipulations (Siddiqi et al. 2022). Thus, in addition to being more comprehensive than previous attempts, the TD-map provides causal evidence for the brain system underlying spatial cognition.

Nevertheless, our methodology has its limitations. While some of the TD case reports include a detailed description of the patient's spatial disorientation, others only mention this deficit briefly. Moreover, most of cases do not include an objective assessment of the navigational abilities in the premorbid state, and even afterward this assessment is often limited to a subjective description. These limitations may contribute to the fact that not all lesions overlapped in a common seed. However, the seed found was located in a major hub of spatial

cognition, supporting the validity of our results. Another limitation is our reliance on 2-dimensional images: 3-dimensional reconstructions were not available and there were variations in the number of images and the level of textual anatomical specifications between the different studies, limiting the precision of our analysis. However, 78% of the cases included several 2-dimensional slices, providing partial information on the third dimension. In addition, in 88% of the cases, the provided images encompassed all the implicated brain structures. When using either only the multi-slice lesions or only the lesions encompassing all implicated structures, results remained equivalent to those of the original analysis. This consistency aligns with prior applications of the lesion network analysis, which have demonstrated that 2-dimensional slices can appropriately approximate the connectivity patterns of a whole 3-dimensional lesion (Boes et al. 2015; Cotovio et al. 2020).

While the functional connectome was derived from subjects younger than our TD cohort, prior work has shown that using an age matched connectome makes little difference in results (Fox et al. 2014; Boes et al. 2015) and many lesion network mapping analyses have relied on normative connectivity data from younger adults to derive network maps of lesions in older adults (Kletenik et al. 2022; Nabizadeh and Aarabi 2023). Finally, our analysis was based on functional connectivity data that was collected during rest and not while navigational task-associated connectivity. Nonetheless, rest may be regarded as a fixation task, and a significant correlation was found between functional connectivity during fixation and during other tasks, presumably enabling inferences from rest- to task-evoked functional connectivity (Tavor et al. 2016).

In conclusion, our results provide a comprehensive map of the brain systems underlying spatial orientation, which includes brain regions that were not considered previously, and may be used in future investigations of spatial cognition.

Funding

The study was supported by the NIH grant no. 124971. M. R. is supported by the VATAT scholarship for Data Science doctoral students.

Acknowledgements

The authors thank Amnon Dafni-Merom for helpful comments on the manuscript.

Correspondence to: Moshe Roseman, Neuropsychiatry Lab, Department of Medical Neurosciences, Faculty of Medicine, Hadassah Hebrew University Medical School, Jerusalem 9112001, Israel

Tel.: +972 2 6777741; fax: +972 2 6437782; email: moshe.roseman@mail.huji.ac.il

References

Aguirre GK, D'Esposito M. Topographical disorientation: a synthesis and taxonomy. Brain. 1999:122(9):1613–1628.

Andrews-Hanna JR, Smallwood J, Spreng RN. The default network and self-generated thought: component processes, dynamic control, and clinical relevance. Ann N Y Acad Sci. 2014:1316(1):29–52.

Arzy S, Kaplan R. Transforming social perspectives with cognitive maps. Soc Cogn Affect Neurosci. 2022:00:1–17.

Arzy S, Schacter DL. Self-Agency and Self-Ownership in Cognitive Mapping. Trends Cogn Sci. 2019:23(6):476–487.

Balaguer J, Spiers H, Hassabis D, Summerfield C. Neural Mechanisms of Hierarchical Planning in a Virtual Subway Network. Neuron. 2016:90(4):893–903.

Behrens TEJ, Muller TH, Whittington JCR, Mark S, Baram AB, Stachenfeld KL, Kurth-Nelson Z. What Is a Cognitive Map? Organizing Knowledge for Flexible Behavior. Neuron. 2018:100(2):490–509.

Bicanski A, Burgess N. A neural-level model of spatial memory and imagery. Elife. 2018:7.

Boes AD, Prasad S, Liu H, Liu Q, Pascual-Leone A, Caviness Jr VS, Fox MD. Network localization of neurological symptoms from focal brain lesions. Brain. 2015:138(10):3061–3075.

Braga RM, Van Dijk KRA, Polimeni JR, Eldaief MC, Buckner RL. Parallel distributed networks resolved at high resolution reveal close juxtaposition of distinct regions. J Neurophysiol. 2019:121(4):1513–1534.

Buckner RL, Andrews-Hanna JR, Schacter DL. The Brain's Default Network: Anatomy, Function, and Relevance to Disease. Ann N Y Acad Sci. 2008:1124(1):1–38.

Buckner RL, Carroll DC. Self-projection and the brain. Trends Cogn Sci. 2007:11(2):49–57.

Buckner RL, Sepulcre J, Talukdar T, Krienen FM, Liu H, Hedden T, Andrews-Hanna JR, Sperling RA, Johnson KA. Cortical Hubs Revealed by Intrinsic Functional Connectivity: Mapping, Assessment of Stability, and Relation to Alzheimer's Disease. J Neurosci. 2009:29(6):1860–1873.

Buckner RL, Snyder AZ, Shannon BJ, LaRossa G, Sachs R, Fotenos AF, Sheline YI, Klunk WE, Mathis CA, Morris JC, et al. Molecular, Structural, and Functional Characterization of

473 Alzheimer's Disease: Evidence for a Relationship between Default Activity, Amyloid, and
474 Memory. J Neurosci. 2005:25(34):7709–7717.

475 Burgess N, Maguire EA, O'Keefe J. The Human Hippocampus and Spatial and Episodic
476 Memory. Neuron. 2002:35(4):625–641.

477 Buzsáki G, Moser EI. Memory, navigation and theta rhythm in the hippocampal-entorhinal
478 system. Nat Neurosci. 2013:16(2):130–138.

479 Byrne P, Becker S, Burgess N. Remembering the past and imagining the future: a neural model
480 of spatial memory and imagery. Psychol Rev. 2007:114(2):340–375.

481 Chadwick MJ, Jolly AEJ, Amos DP, Hassabis D, Spiers HJ. A Goal Direction Signal in the
482 Human Entorhinal/Subicular Region. Curr Biol. 2015:25(1):87–92.

483 Chrastil ER, Sherrill KR, Aselcioglu I, Hasselmo ME, Stern CE. Individual Differences in
484 Human Path Integration Abilities Correlate with Gray Matter Volume in Retrosplenial Cortex,
485 Hippocampus, and Medial Prefrontal Cortex. eNeuro. 2017:4(2):ENEURO.0346-16.2017.

486 Ciaramelli E. The role of ventromedial prefrontal cortex in navigation: A case of impaired
487 wayfinding and rehabilitation. Neuropsychologia. 2008:46(7):2099–2105.

488 Cohen AL, Soussand L, Corrow SL, Martinaud O, Barton JJS, Fox MD. Looking beyond the
489 face area: lesion network mapping of prosopagnosia. Brain. 2019:142(12):3975–3990.

490 Corp DT, Joutsa J, Darby RR, Delnooz CCS, Van De Warrenburg BPC, Cooke D, Prudente
491 CN, Ren J, Reich MM, Batla A, et al. Network localization of cervical dystonia based on causal
492 brain lesions. Brain. 2019:142(6):1660–1674.

493 Cotovio G, Talmasov D, Bernardo Barahona-Corrêa J, Hsu J, Senova S, Ribeiro R, Soussand
494 L, Velosa A, Cruz e Silva V, Rost N, et al. Mapping mania symptoms based on focal brain
495 damage. J Clin Invest. 2020:130(10):5209–5222.

Coughlan G, Laczó J, Hort J, Minihane AM, Hornberger M. Spatial navigation deficits — Overlooked cognitive marker for preclinical Alzheimer disease? Nat Rev Neurol. 2018:14(8):496–506.

Dafni-Merom A, Arzy S. The radiation of autonoetic consciousness in cognitive neuroscience: A functional neuroanatomy perspective. Neuropsychologia. 2020:143:107477.

Dafni-Merom A, Peters-Founshtein G, Kahana-Merhavi S, Arzy S. A unified brain system of orientation and its disruption in Alzheimer's disease. Ann Clin Transl Neurol. 2019:6(12):2468–2478.

Darby RR, Horn A, Cushman F, Fox MD. Lesion network localization of criminal behavior. Proc Natl Acad Sci. 2018:115(3):601 LP – 606.

Darby RR, Joutsa J, Burke MJ, Fox MD. Lesion network localization of free will. Proc Natl Acad Sci U S A. 2018:115(42):10792–10797.

Darby RR, Joutsa J, Fox MD. Network localization of heterogeneous neuroimaging findings. Brain. 2019:142(1):70–79.

Dilks DD, Julian JB, Paunov AM, Kanwisher N. The Occipital Place Area Is Causally and Selectively Involved in Scene Perception. J Neurosci. 2013:33(4):1331–1336.

DiNicola LM, Braga RM, Buckner RL. Parallel distributed networks dissociate episodic and social functions within the individual. J Neurophysiol. 2020:123(3):1144–1179.

Doeller CF, Barry C, Burgess N. Evidence for grid cells in a human memory network. Nature. 2010:463(7281):657–661.

Epstein R, Kanwisher N. A cortical representation of the local visual environment. Nature. 1998:392(6676):598–601.

518 Epstein RA, Parker WE, Feiler AM. Where Am I Now? Distinct Roles for Parahippocampal
519 and Retrosplenial Cortices in Place Recognition. J Neurosci. 2007:27(23):6141–6149.

520 Epstein RA, Patai EZ, Julian JB, Spiers HJ. The cognitive map in humans: spatial navigation
521 and beyond. Nat Neurosci. 2017:20:1504.

522 Farzanfar D, Spiers HJ, Moscovitch M, Rosenbaum RS. From cognitive maps to spatial
523 schemas. Nat Rev Neurosci. 2022:24(2):63–79.

524 Fasano A, Laganiere SE, Lam S, Fox MD. Lesions causing freezing of gait localize to a
525 cerebellar functional network. Ann Neurol. 2017:81(1):129–141.

526 Ferguson MA, Lim C, Cooke D, Darby RR, Wu O, Rost NS, Corbetta M, Grafman J, Fox MD.
527 A human memory circuit derived from brain lesions causing amnesia. Nat Commun.
528 2019:10(1):1–9.

529 Ferguson MA, Schaper FLWVJ, Cohen A, Siddiqi S, Merrill SM, Nielsen JA, Grafman J,
530 Urgesi C, Fabbro F, Fox MD. A Neural Circuit for Spirituality and Religiosity Derived From
531 Patients With Brain Lesions. Biol Psychiatry. 2021:91(4):380–388.

532 Fox MD. Mapping Symptoms to Brain Networks with the Human Connectome. N Engl J Med.
533 2018:379(23):2237–2245.

534 Fox MD, Buckner RL, Liu H, Chakravarty MM, Lozano AM, Pascual-Leone A. Resting-state
535 networks link invasive and noninvasive brain stimulation across diverse psychiatric and
536 neurological diseases. Proc Natl Acad Sci. 2014:111(41):E4367–E4375.

537 Frings L, Wagner K, Quiske A, Schwarzwald R, Spreer J, Halsband U, Schulze-Bonhage A.
538 Precuneus is involved in allocentric spatial location encoding and recognition. Exp Brain Res.
539 2006:173(4):661–672.

540 Ghaem O, Mellet E, Crivello F, Tzourio N, Mazoyer B, Berthoz A, Denis M. Mental navigation

along memorized routes activates the hippocampus, precuneus, and insula. Neuroreport. 1997:8(3):739–744.

Gordon EM, Laumann TO, Adeyemo B, Huckins JF, Kelley WM, Petersen SE. Generation and Evaluation of a Cortical Area Parcellation from Resting-State Correlations. Cereb Cortex. 2016:26(1):288–303.

Greicius MD, Srivastava G, Reiss AL, Menon V. Default-mode network activity distinguishes Alzheimer's disease from healthy aging: Evidence from functional MRI. Proc Natl Acad Sci U S A. 2004:101(13):4637–4642.

Habib M, Sirigu A. Pure Topographical Disorientation: A Definition and Anatomical Basis. Cortex. 1987:23(1):73–85.

van der Ham IJM, Martens MAG, Claessen MHG, van den Berg E. Landmark Agnosia: Evaluating the Definition of Landmark-based Navigation Impairment. Arch Clin Neuropsychol. 2017:32(4):472–482.

Hartley T, Lever C, Burgess N, O'Keefe J. Space in the brain: how the hippocampal formation supports spatial cognition. Philos Trans R Soc B Biol Sci. 2014:369(1635).

Hashimoto R, Tanaka Y, Nakano I. Heading Disorientation: A New Test and a Possible Underlying Mechanism. Eur Neurol. 2010:63(2):87–93.

Hassabis D, Maguire EA. Deconstructing episodic memory with construction. Trends Cogn Sci. 2007:11(7):299–306.

Horner AJ, Bisby JA, Zotow E, Bush D, Burgess N. Grid-like Processing of Imagined Navigation. Curr Biol. 2016:26(6):842–847.

Javadi AH, Patai EZ, Marin-Garcia E, Margolis A, Tan HRM, Kumaran D, Nardini M, Penny W, Duzel E, Dayan P, et al. Prefrontal Dynamics Associated with Efficient Detours and

564 Shortcuts: A Combined Functional Magnetic Resonance Imaging and
565 Magnetoencenphalography Study. J Cogn Neurosci. 2019:31(8):1227–1247.

566 Joutsa J, Horn A, Hsu J, Fox MD. Localizing parkinsonism based on focal brain lesions. Brain.
567 2018:141(8):2445–2456.

568 Joutsa J, Shih LC, Fox MD. Mapping holmes tremor circuit using the human brain connectome.
569 Ann Neurol. 2019:86(6):812–820.

570 Julian JB, Fedorenko E, Webster J, Kanwisher N. An algorithmic method for functionally
571 defining regions of interest in the ventral visual pathway. Neuroimage. 2012:60(4):2357–2364.

572 Kaplan R, King J, Koster R, Penny WD, Burgess N, Friston KJ. The Neural Representation of
573 Prospective Choice during Spatial Planning and Decisions. PLOS Biol. 2017:15(1):e1002588.

574 Kletenik I, Cohen AL, Glanz BI, Ferguson MA, Tauhid S, Li J, Drew W, Polgar-Turcsanyi M,
575 Palotai M, Siddiqi SH. Multiple sclerosis lesions that impair memory map to a connected
576 memory circuit. J Neurol. 2023:270(11):5211–5222.

577 Kletenik I, Ferguson MA, Bateman JR, Cohen AL, Lin C, Tetreault A, Pelak VS, Anderson
578 CA, Prasad S, Darby RR, et al. Network Localization of Unconscious Visual Perception in
579 Blindsight. Ann Neurol. 2022:91(2):217–224.

580 Kletenik I, Gaudet K, Prasad S, Cohen AL, Fox MD. Network Localization of Awareness in
581 Visual and Motor Anosognosia. Ann Neurol. 2023.

582 Kumaran D, Banino A, Blundell C, Hassabis D, Dayan P. Computations Underlying Social
583 Hierarchy Learning: Distinct Neural Mechanisms for Updating and Representing Self-
584 Relevant Information. Neuron. 2016:92(5):1135–1147.

585 Kunz L, Schröder TN, Lee H, Montag C, Lachmann B, Sariyska R, Reuter M, Stirnberg R,
586 Stöcker T, Messing-Floeter PC, et al. Reduced grid-cell-like representations in adults at genetic

risk for Alzheimer's disease. Science (80-). 2015:350(6259):430–433.

Laganiere S, Boes AD, Fox MD. Network localization of hemichorea-hemiballismus. Neurology. 2016:86(23):2187–2195.

Lambrey S, Doeller C, Berthoz A, Burgess N. Imagining Being Somewhere Else: Neural Basis of Changing Perspective in Space. Cereb Cortex. 2012:22(1):166–174.

Maguire E. The retrosplenial contribution to human navigation: A review of lesion and neuroimaging findings. Scand J Psychol. 2001:42(3):225–238.

Marchette SA, Vass LK, Ryan J, Epstein RA. Outside Looking In: Landmark Generalization in the Human Navigational System. J Neurosci. 2015:35(44):14896–14908.

Marcus D, Harwell J, Olsen T, Hodge M, Glasser M, Prior F, Jenkinson M, Laumann T, Curtiss S, Van Essen D. Informatics and Data Mining Tools and Strategies for the Human Connectome Project. Front Neuroinform. 2011:5:4.

Margulies DS, Ghosh SS, Goulas A, Falkiewicz M, Huntenburg JM, Langs G, Bezgin G, Eickhoff SB, Castellanos FX, Petrides M, et al. Situating the default-mode network along a principal gradient of macroscale cortical organization. Proc Natl Acad Sci U S A. 2016:113(44):12574–12579.

Nabizadeh F, Aarabi MH. Functional and Structural Lesion network mapping in Neurological and psychiatric disorders: a systematic review. Front Neurol. 2023:14:1100067.

O'Keefe J, Nadel L. The hippocampus as a cognitive map. Oxford: Clarendon Press.

Padmanabhan JL, Cooke D, Joutsa J, Siddiqi SH, Ferguson M, Darby RR, Soussand L, Horn A, Kim NY, Voss JL, et al. A Human Depression Circuit Derived From Focal Brain Lesions. Biol Psychiatry. 2019:86(10):749–758.

609 Park SA, Miller DS, Nili H, Ranganath C, Boorman ED. Map Making: Constructing,
610 Combining, and Inferring on Abstract Cognitive Maps. Neuron. 2020:0(0).

611 Patai EZ, Javadi A-H, Ozubko JD, O'Callaghan A, Ji S, Robin J, Grady C, Winocur G,
612 Rosenbaum RS, Moscovitch M, et al. Hippocampal and Retrosplenial Goal Distance Coding
613 After Long-term Consolidation of a Real-World Environment. Cereb Cortex.
614 2019:29(6):2748–2758.

615 Patai EZ, Spiers HJ. The Versatile Wayfinder: Prefrontal Contributions to Spatial Navigation.
616 Trends Cogn Sci. 2021:25(6):520–533.

617 Peer M, Ron Y, Monsa R, Arzy S. Processing of different spatial scales in the human brain.
618 Elife. 2019:8.

619 Peer M, Salomon R, Goldberg I, Blanke O, Arzy S. Brain system for mental orientation in
620 space, time, and person. Proc Natl Acad Sci U S A. 2015:112(35):11072–7.

621 Peters-Founshtein G, Peer M, Rein Y, Kahana-Merhavi S, Meiner Z, Arzy S. Mental-
622 orientation: A new approach to assessing patients across the Alzheimer's disease spectrum.
623 Neuropsychology. 2018:32(6):690–699.

624 Ranganath C, Ritchey M. Two cortical systems for memory-guided behaviour. Nat Rev
625 Neurosci. 2012:13(10):713–726.

626 Ruby P, Decety J. Effect of subjective perspective taking during simulation of action: a PET
627 investigation of agency. Nat Neurosci. 2001:4(5):546–550.

628 Sherrill KR, Erdem UM, Ross RS, Brown TI, Hasselmo ME, Stern CE. Hippocampus and
629 Retrosplenial Cortex Combine Path Integration Signals for Successful Navigation. J Neurosci.
630 2013:33(49):19304–19313.

631 Siddiqi SH, Kording KP, Parvizi J, Fox MD. Causal mapping of human brain function. Nat

Rev Neurosci. 2022:23(6):361–375.

Son J-Y, Bhandari A, FeldmanHall O. Cognitive maps of social features enable flexible inference in social networks. Proc Natl Acad Sci. 2021:118(39).

Spiers HJ, Maguire EA. Thoughts, behaviour, and brain dynamics during navigation in the real world. Neuroimage. 2006:31(4):1826–1840.

Spreng RN, Mar RA, Kim ASN. The common neural basis of autobiographical memory, prospection, navigation, theory of mind, and the default mode: A quantitative meta-analysis. J Cogn Neurosci. 2009:21(3):489–510.

Stark M, Coslett HB, Saffran EM. Impairment of an Egocentric Map of Locations: Implications for Perception and Action. Cogn Neuropsychol. 1996:13(4):481–524.

Takahashi N, Kawamura M. Pure Topographical Disorientation —The Anatomical Basis of Landmark Agnosia. Cortex. 2002:38(5):717–725.

Tavares RM, Mendelsohn A, Grossman Y, Williams CH, Shapiro M, Trope Y, Schiller D. A Map for Social Navigation in the Human Brain. Neuron. 2015:87(1):231–243.

Tavor I, Parker Jones O, Mars RB, Smith SM, Behrens TE, Jbabdi S. Task-free MRI predicts individual differences in brain activity during task performance. Science (80-). 2016:352(6282):216–220.

Tolman EC. Cognitive maps in rats and men. Psychol Rev. 1948:55(4):189–208.

Vann SD, Aggleton JP, Maguire EA. What does the retrosplenial cortex do? Nat Rev Neurosci. 2009:10(11):792–802.

Vogeley K, Fink GR. Neural correlates of the first-person-perspective. Trends Cogn Sci. 2003:7(1):38–42.

654 Wolbers T, Wiener JM, Mallot HA, Büchel C. Differential Recruitment of the Hippocampus,
655 Medial Prefrontal Cortex, and the Human Motion Complex during Path Integration in Humans.
656 J Neurosci. 2007:27(35):9408–9416.

657 Yan C, Zang Y. DPARSF: a MATLAB toolbox for "pipeline" data analysis of resting-state
658 fMRI. Front Syst Neurosci. 2010:4:13.

659 Yeo BTT, Krienen FM, Sepulcre J, Sabuncu MR, Lashkari D, Hollinshead M, Roffman JL,
660 Smoller JW, Zöllei L, Polimeni JR, et al. The organization of the human cerebral cortex
661 estimated by intrinsic functional connectivity. J Neurophysiol. 2011:106(3):1125–1165.

662

663 Figures

664

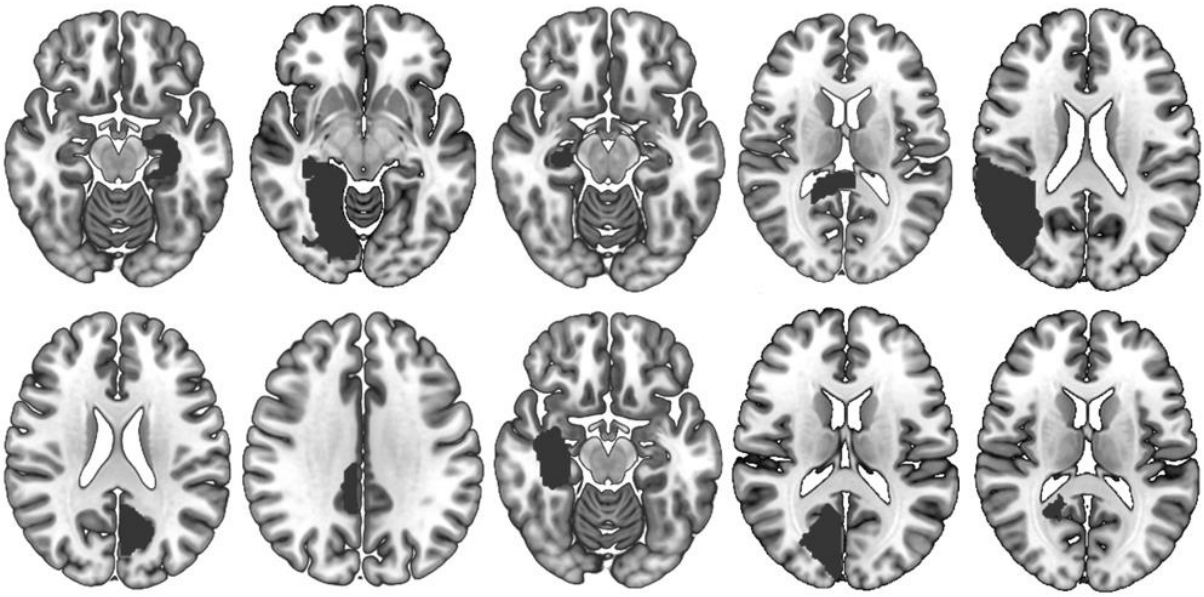

665
666 **Figure 1 Ten examples of lesions causing topographical disorientation (from a total**
667 **sample of 65).**

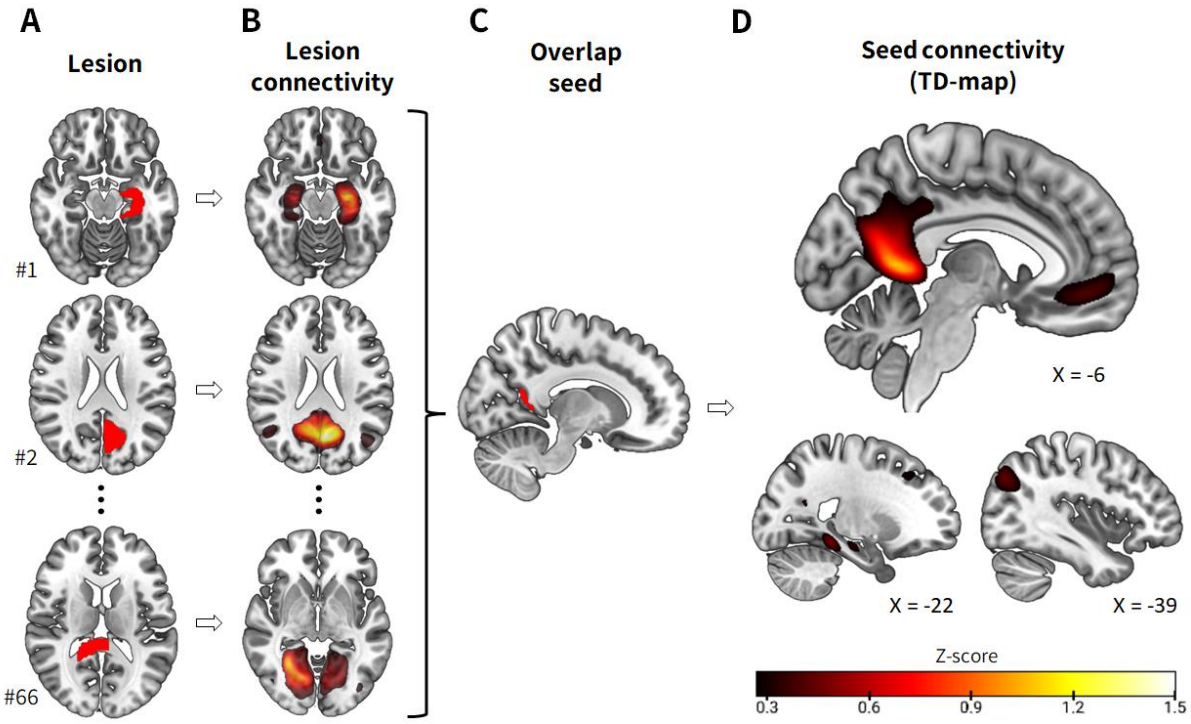

Figure 2 Functional connectivity of lesions causing topographical disorientation yields a common brain circuit. (A) 65 lesions in various brain regions were manually extracted from neuroimages in case reports of topographical disorientation. **(B)** A functional connectivity map was calculated for each lesion based on resting-state functional magnetic resonance imaging (fMRI) data of 1,000 healthy volunteers. **(C)** The maximal overlap between connectivity maps (41 maps) was found in the parieto-occipital sulcus. **(D)** A brain circuit of topographical disorientation (TD-map) was identified based on the functional connectivity of the overlap seed using the same resting-state fMRI database. For full details of the implicated brain regions, see Table 1.

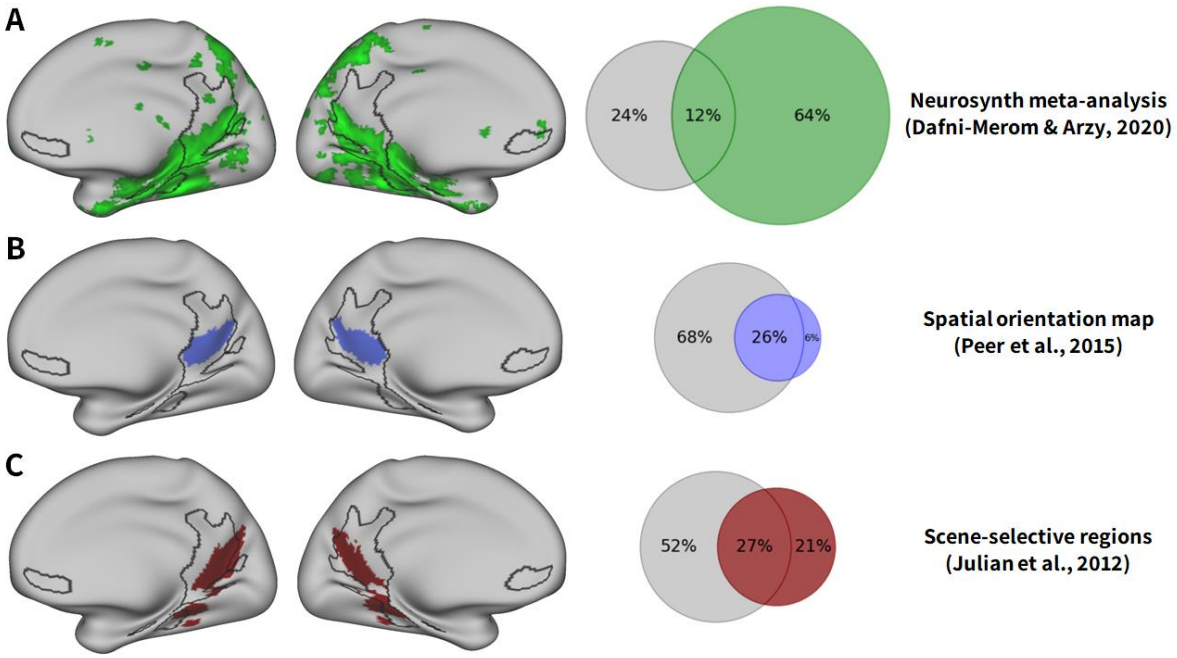

Figure 3 The topographical disorientation lesion network map (TD-map, outlined in black) and other brain maps of spatial cognition with Venn diagrams illustrating overlap. **(A)** a meta-analysis of navigation-related fMRI experiments, performed via the Neurosynth database (green), overlaps partially with the TD-map; note that the PCC and the mPFC are included in the TD-map but not in the meta-analysis results. **(B)** The spatial orientation mask (Peer et al. 2015) (blue) is contained almost entirely within the TD-map. **(C)** When comparing to the scene-selective brain regions (Julian et al. 2012) (brown), the RSC and the PPA significantly overlap with the TD-map (75% of the RSC region, 31% of the PPA); as for the third scene-selective region (OPA) in the lateral occipital lobe (not shown), only 15% of the region overlapped with the TD-map.

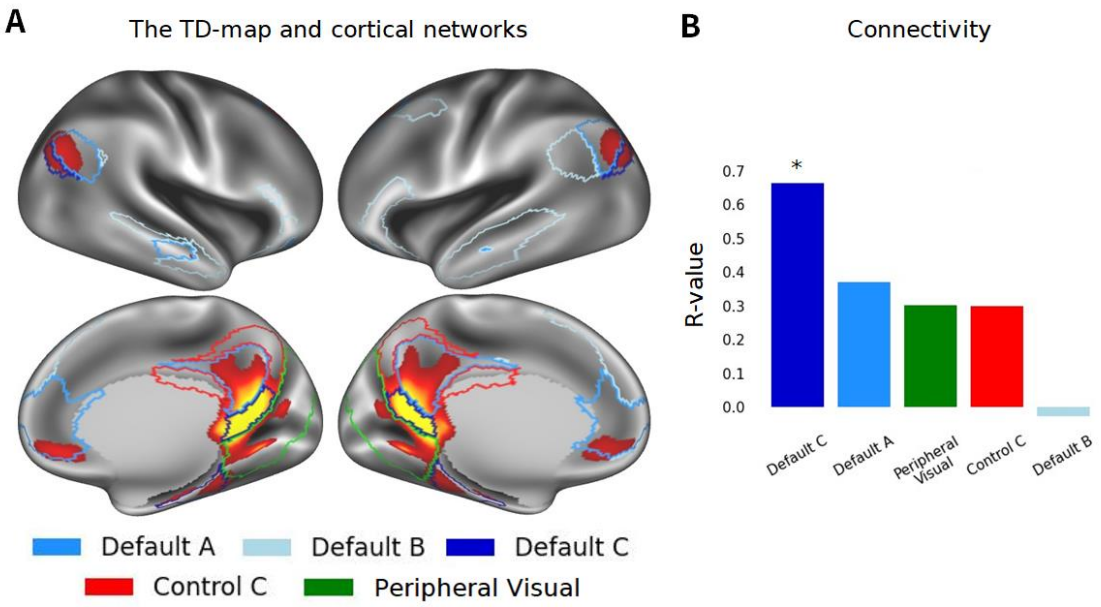

691

692 **Figure 4 Overlap and connectivity between the TD-map and cortical networks. (A)** The
693 TD-map (orange-yellow) is shown with respect to cortical subnetworks (Yeo et al. 2011),
694 including DMN subnetworks (Default C, dark-blue; Default A, blue; Default B, light-blue) and
695 two other cortical networks which overlapped with it (Peripheral Visual, green; Control C, red).
696 **(B)** Functional connectivity between the implicated cortical networks and the TD-map. * $p \leq$
697 0.05, corrected for all 17 networks.

698

699

700